A converted-wave experiment in Uganda

J. Helen Isaac, Francesca Martini and Gary Margrave

ABSTRACT

We processed an experimental 3C survey acquired in Uganda. There was concern that the azimuths of the 3C geophones were not exactly as planned, which was magnetic north, since the geophones had been dropped into holes. The results of rotation analysis on the data were inconsistent and we considered that they deviated too much from the planned field orientation to be used. We rotated the data using a constant receiver orientation of magnetic north.

The PS data image the acoustic basement well but reflections shallower in the section have less continuity and are of lower amplitude. The PP data show more structure on the basement reflector and much better resolution of reflectors above basement. We picked two horizons on the migrated PP and PS sections by correlating first the basement reflectors then picking a shallower horizon on the PS data and matching that to the PP data. The values of Vp/Vs calculated from the interval traveltimes measured on the PP and PS data were consistent with Vp/Vs values of 3.0 – 3.4 measured on logs from a nearby well.

INTRODUCTION

In 2010, a 3C seismic survey was acquired as part of a wider exploration program in the lake Albert Rift Basin of Uganda to test the value of 3C data in this area. This intra-continental rift basin contains low velocity Miocene clastic sediments in which there are multiple pay zones of oil and gas. Although the basement is highly faulted in the rift valley, it is relatively undeformed in the vicinity of the short 3C line and occurs at a seismic reflection time of about 1 second.

The source for the line was dynamite spaced at 25 m station intervals. The 158 2-Hz geophones were laid out as a secondary recording system alongside conventional 1C instruments but at half their spacing, at 12.5 m station intervals, and buried 30 cm deep. For this study, only those shots from locations corresponding to the surface location of the 3C receivers were processed; a total of 80.

DATA PROCESSING

Vertical component

The vertical component was processed first through a standard processing scheme, which included amplitude scaling, noise attenuation, deconvolution and bandpass filter to enhance the data while elevation statics, first break statics and residual statics improved the continuity of reflectors. Some of the shots had greatly delayed arrival times due to recording error and had hand-calculated statics applied prior to any processing. The shot statics were summed for each station and exported from the database for import into the radial component database.

An example of a shot gather before and after amplitude scaling, noise attenuation is given in Figure 1, where we display the first 2 s of data. The same gather with Gabor deconvolution (Margrave and Lamoureux, 2002; Margrave et al., 2003) applied is shown in Figure 2. Figure 3 shows the stacked data. The strong reflector seen just below 0.8 s is believed to be acoustic basement. This section was post-stack time migrated (Figure 4) but no pre-stack migrations were performed at this time.
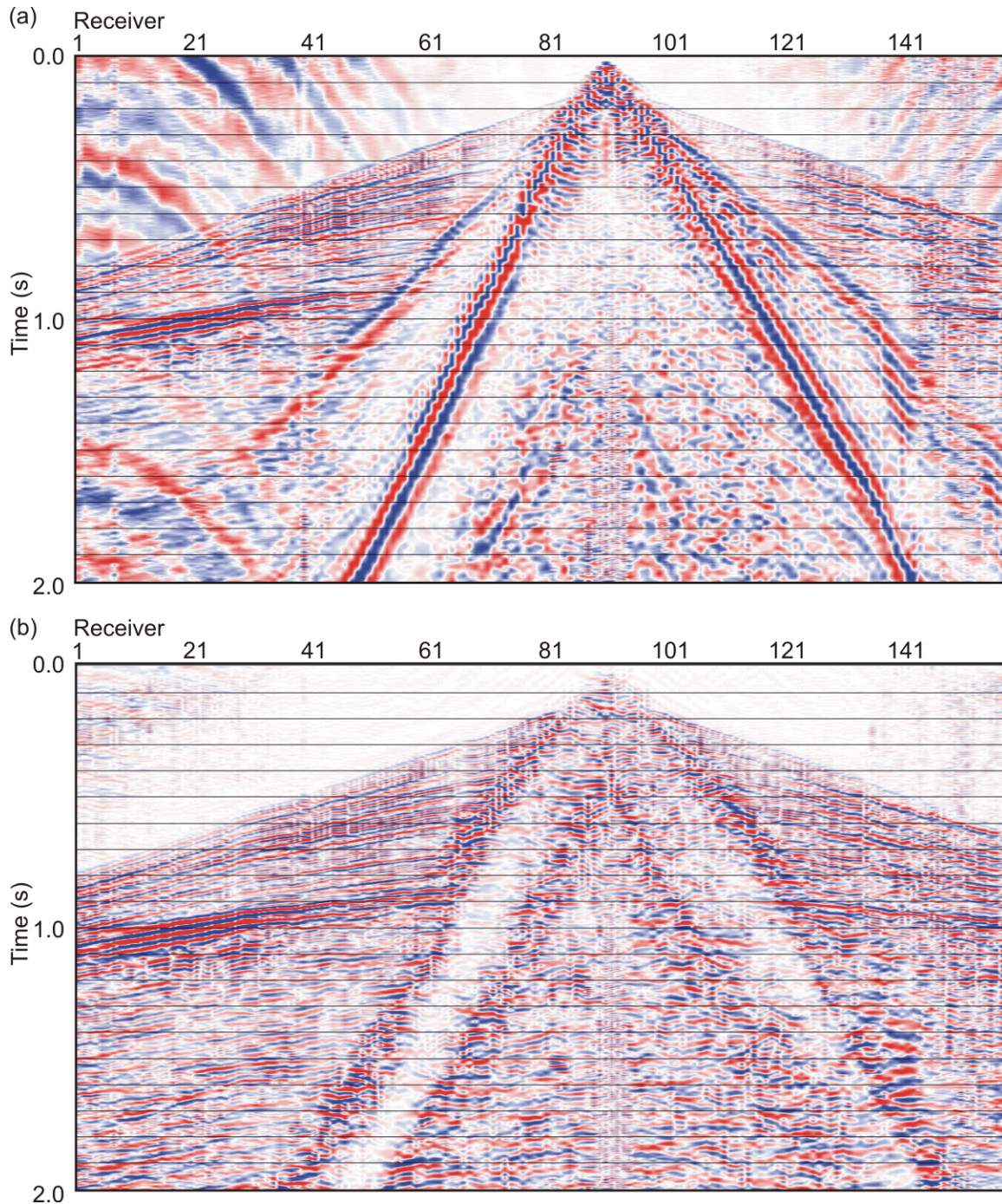

FIG. 1. (a) Field shot gather (with AGC applied for display only). (b) The same gather after processing to attenuate noise and enhance signal.
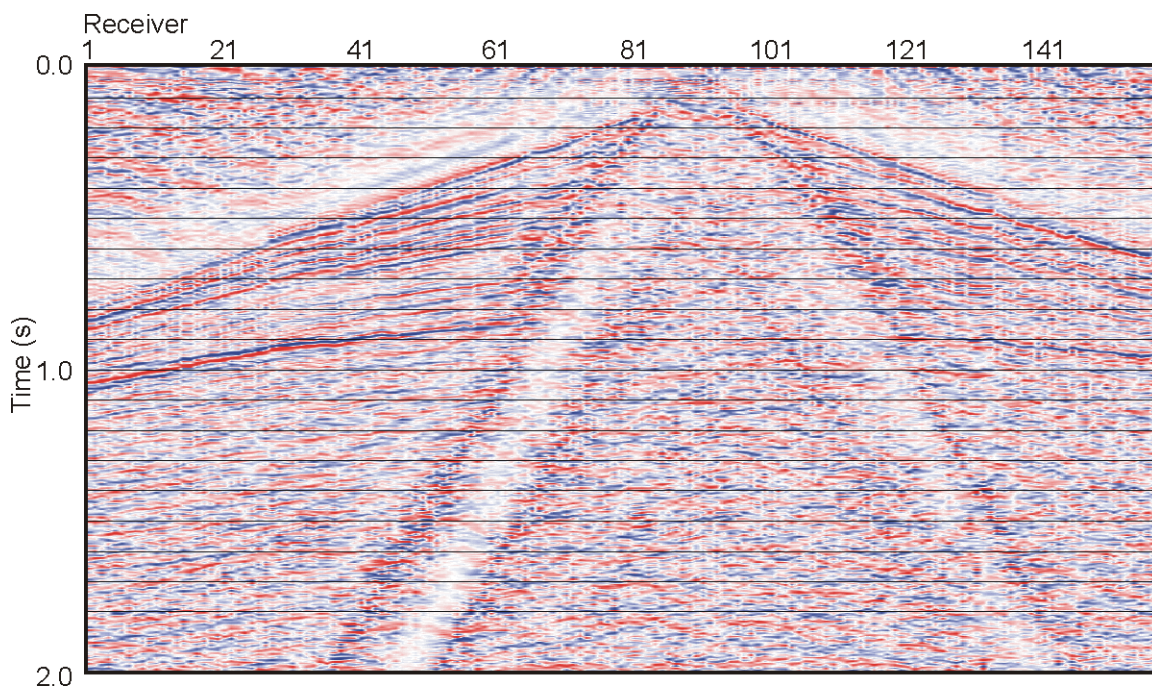
FIG. 2. The same shot gather as in Figure 1 with Gabor deconvolution applied.
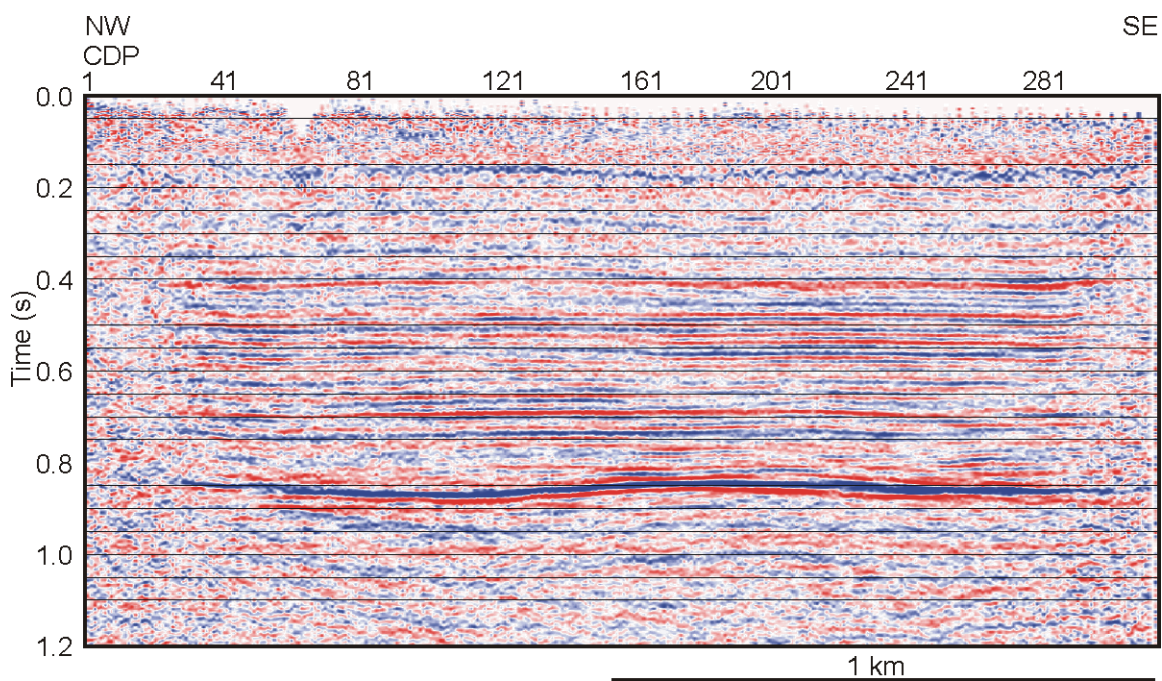

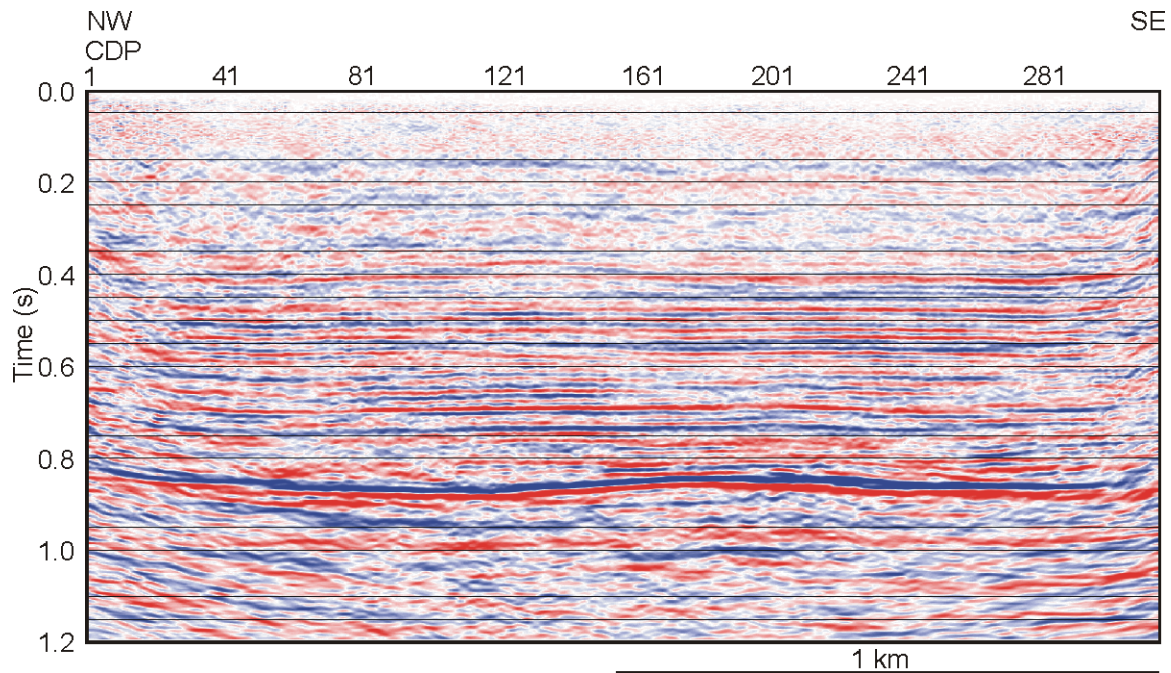FIG. 3. Stacked vertical component. Blue represents a peak.

FIG. 4. Poststack migrated version of the stack shown in Figure 3.

Horizontal components

The horizontal components H1 and H2 recorded in the field were identified by the header words geo_comp 2 and geo_comp 3. In Figure 5 the shot gathers from the two components, H1 and H2, exhibit opposite polarities for the positive and negative offsets and opposite polarities to each other. It was planned that the geophones would be laid out in a geographical orientation: magnetic north for H1 and east for H2. This orientation of north and east correlates with the observed reversal of polarity between the two horizontal components and on the leading and trailing spreads.

Since the geophones had been dropped into the holes, the orientation may not have remained exactly magnetic north. Therefore, we performed rotation analysis on the data to try to determine the exact original geophone azimuth. The data were sorted into receiver gathers and a subset of offsets with good first break arrivals (0-1000 m) was selected. The automatic receiver orientation analysis calculated the original azimuth based upon rotation of the components such that the maximum horizontal energy appears on the rotated H1 component. In Promax the analysis assumes H2 to be 90° anticlockwise of H1, which is opposite to the normal deployment, so we had to reverse the polarity of all the H2 traces. The analysis was performed for every receiver with groups of three traces representing the three components from each shot. First we subtracted 180° from angles between 91° and 269° and 360° from angles between 270° and 360° so that the values ranged between -90° and +90° then averaged the results from all shots for each receiver station. The resulting original H1 azimuths were inconsistent (Figure 6), as were the individual results for the shots averaged into each receiver. Since the values were inconsistent and varied from magnetic north (unacceptably much for some receivers), we considered the results to be unreliable for this particular dataset. Thus we rotated the

components with the constant value of magnetic north. The rotations of H1 and H2 into the radial and transverse components were calculated using the equations (1):

$$R = H1\cos\theta + H2\sin\theta$$

$$T = H1\sin\theta - H2\cos\theta \qquad (1)$$

where θ is the angle between the source-receiver azimuth and original H1 azimuth (magnetic north), R is the rotated radial component and T is the rotated transverse component (Figure 7).

These equations take into account the direction of propagation and result in traces that have positive polarity in the source-receiver direction.

Figure 8 shows the H1, H2, radial and transverse components of the same shot gather. We observe that the converted-wave energy between 2.0 and 2.4 s has been concentrated on the radial component and that all traces have the same polarity.
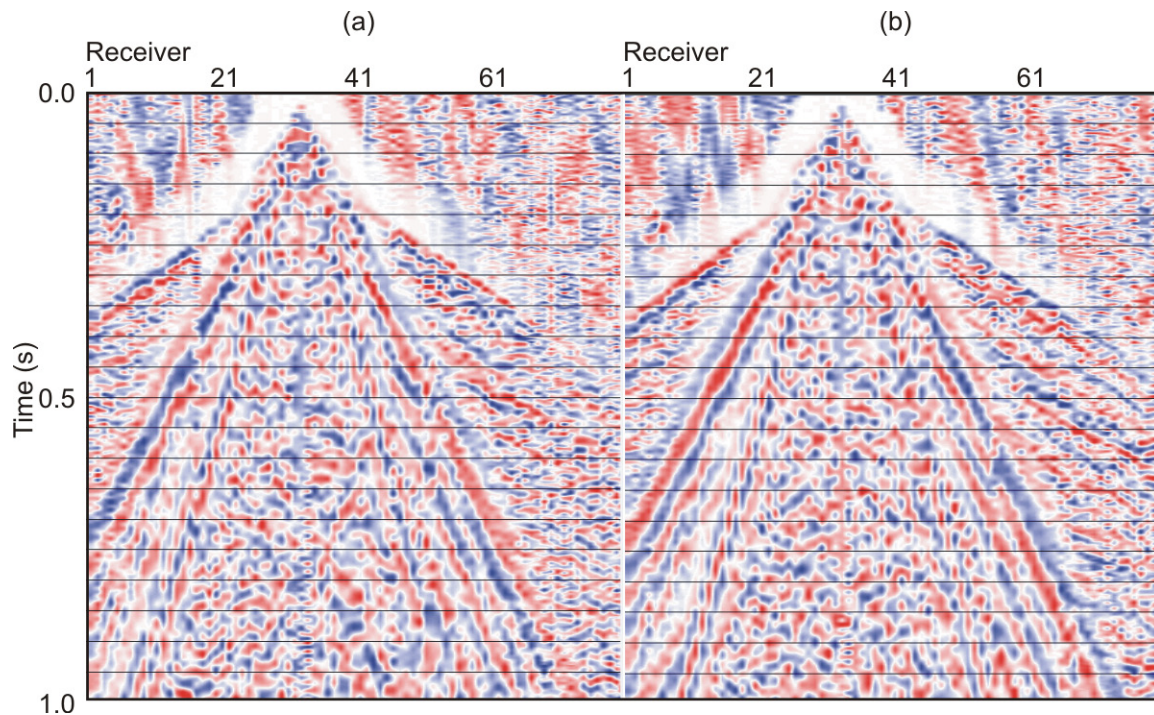

FIG. 5. Part of a shot gather from the (a) H1 component and (b) H2 component of the 3C data. Note the polarity reversal of the first breaks for the leading and trailing spread on each gather and the polarity reversal between the two gathers.
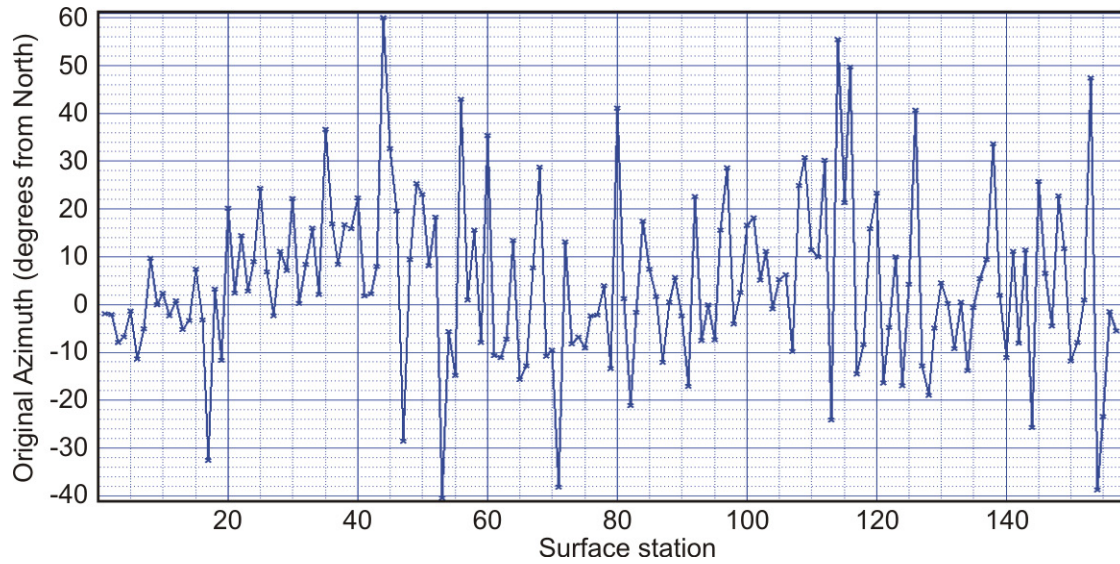
FIG. 6. The original geophone orientation calculated by rotation analysis for each receiver.
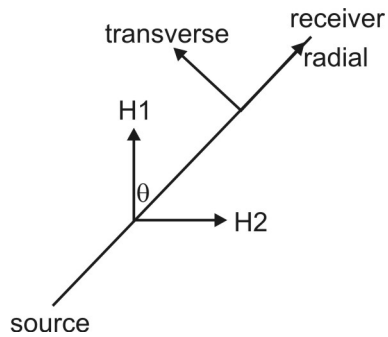

FIG. 7. Rotation of H1 and H2 components into radial and transverse components.
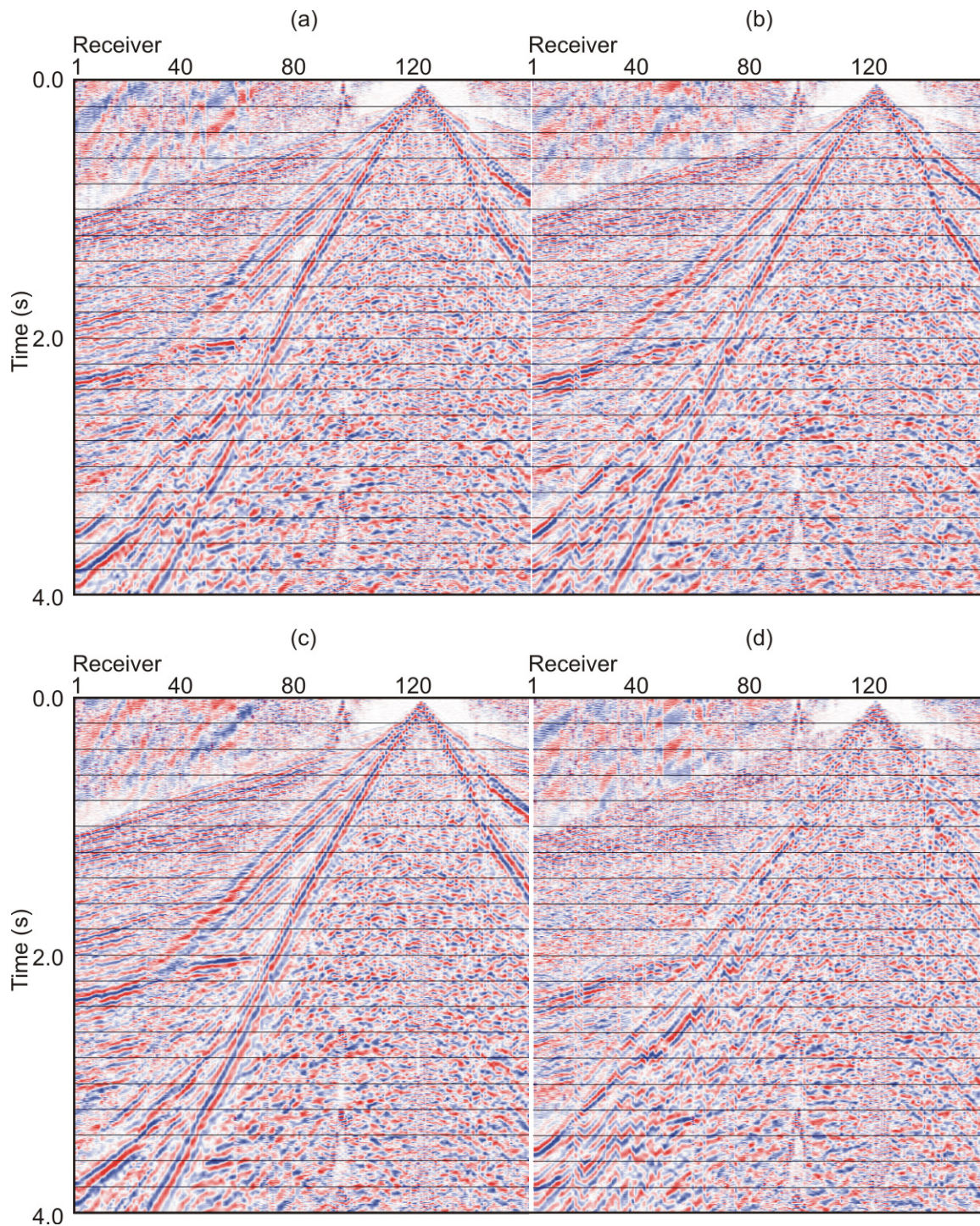
FIG. 8. (a) H1 component, (b) H2 component, (c) radial component and (d) transverse component for a single shot.

The radial component data were processed to attenuate noise and enhance signal. This data enhancement was performed on receiver gathers rather than shot gathers. We applied the shot statics calculated for the vertical component. Receiver statics can be estimated in various ways (Cary and Eaton, 1993; Chan and Stewart, 1997; Li, 2002; Cui et al., 2009; Henley, 2010) but we chose to estimate them by picking a horizon on the stacked receiver gathers, smoothing it, and calculating the static difference between the picked horizon and the smoothed horizon. This difference was also smoothed a little. The amount of smoothing to apply was assessed by the quality of the resulting CCP stack. The estimation of the receiver statics was difficult and there may still be some statics issues with the PS data.

The data were binned into common conversion point (CCP) bins using a Vp/Vs of 3.5, which was estimated from the arrival times of the basement reflector on the PP and PS receiver stacks, and stacked. Figure 9 shows the CCP stack with a post-stack f-x deconvolution applied and Figure 10 is the post-stack migrated section. The acoustic basement reflector shows up well but the reflectors in the section above it are discontinuous and of lower amplitude. The basement reflector does not show as much structure as on the PP section (Figure 4). This could be a velocity effect on the PP data or the result of inaccurate receiver statics on the PS data.

Finally we present the migrated PP and PS sections with the PS section scaled in time to match the basement reflectors (Figure 11). The PP section was bandpass filtered to match better the frequency content of the PS data. We picked two horizons on each section and calculated Vp/Vs from the interval traveltimes between these horizons using equation (2):

$$Vp/Vs = (2\Delta ts/\Delta tp) - 1 \qquad (2)$$

where Δts and Δtp are the PS and PP interval transit times, respectively.

These values of Vp/Vs are plotted beneath the sections. They match the Vp/Vs obtained in a nearby well. CREWES did not have access to these well logs to create synthetic seismograms to match with more confidence the reflectors on the sections. A synthetic would be very useful for identifying the many reflectors on the PP data. The drop in Vp/Vs seen in the NW end of the section is caused by the increased PP traveltime in that area. The PS data do not exhibit as much structure on the acoustic basement as do the PP.
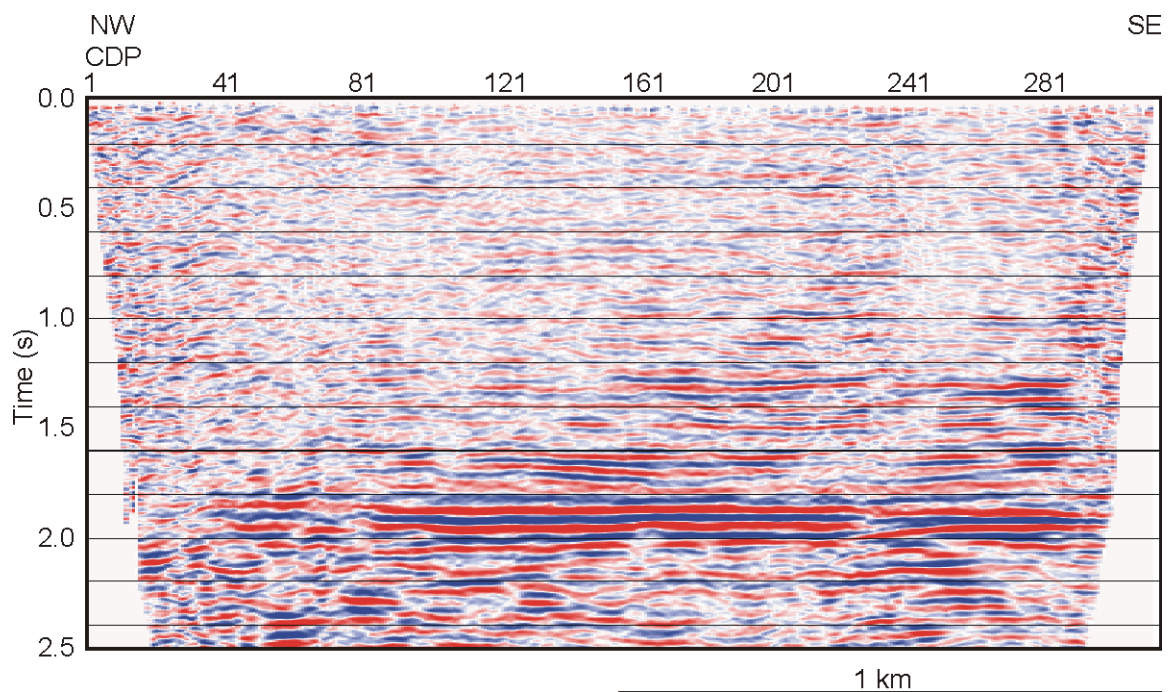
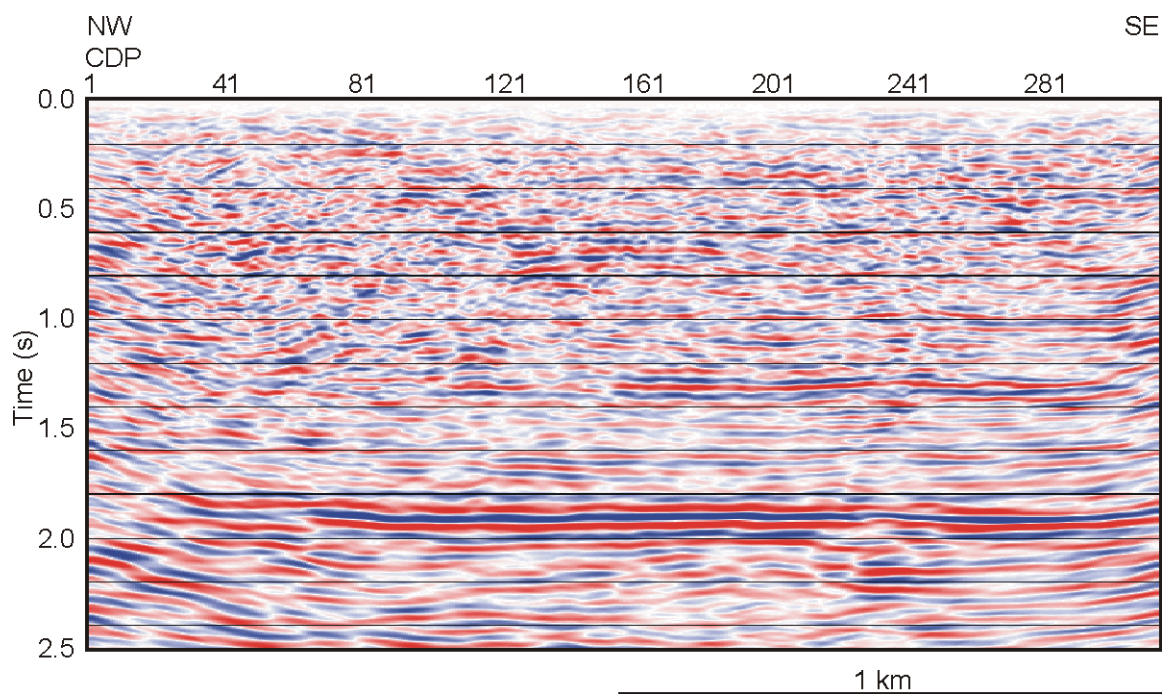FIG. 9. CCP stack with a post-stack f-x deconvolution.

FIG. 10. Migrated version of the stack in Figure 9.

SUMMARY

We processed an experimental 3C survey from Uganda. We attempted to recover the precise orientation of the 3C geophones by rotation analysis on the data. However, the results were inconsistent and we considered that they deviated too much from the planned field orientation, which was magnetic north. Thus we rotated the data using a constant receiver orientation of magnetic north.

On the PS data the acoustic basement is imaged well but reflections shallower in the section have less continuity and are of lower amplitude. There is one horizon at about 1.3 s which we are able to pick. The PP data show more structure on the basement reflector and much better resolution of reflectors above basement. We picked two horizons on the migrated PP and PS sections by correlating first the basement reflectors then picking the shallower horizon on the PS data and matching that as well as we could to the PP data. We recommend use of synthetic seismograms to properly correlate the reflectors. The values of Vp/Vs obtained were consistent with Vp/Vs values of 3.0 – 3.4 measured on logs from a nearby well.
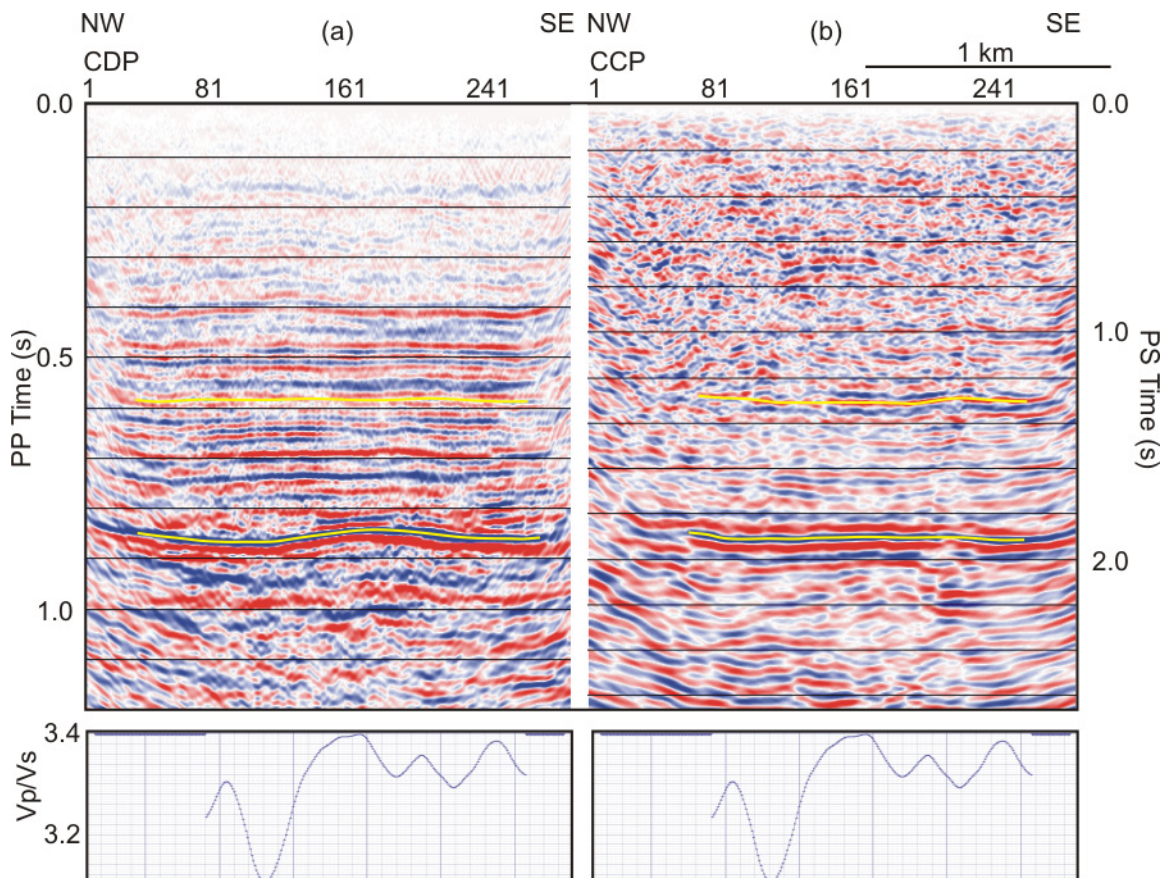

FIG. 11. PP migrated section (a) and PS migrated section (b). The PS section has been scaled in time so that the basement reflectors line up. Vp/Vs is calculated from the interval traveltimes of the two displayed horizons.

ACKNOWLEDGEMENTS

REFERENCES

Cary, P. and D. Eaton, 1993, A simple method for resolving large converted-wave (P-SV) statics: Geophysics, vol. **58**, 429-433.

Chan, W-K. and R. Stewart, 1997, F-x statics for P-S seismic data, CREWES Research Report, vol. 9, 24.1-24.22.

Cui, S., Z. Deng, Y. He, X. Zou and G. Zhao, 2009, On-land converted wave static correction, 71st EAGE conference and exhibition, Amsterdam, The Netherlands, Abstracts.

Henley, D. C., 2010, Correcting PS receiver statics using hybrid raypath interferometry, GeoCanada 2010, Expanded Abstracts.

Li, Y., 2002, A new method for converted wave statics correction, SEG International Exposition and 72nd annual meeting, Salt Lake City, Abstracts.

Margrave, G. F. and M. P. Lamoureux, 2002, Gabor deconvolution: 2002 CSEG Annual Convention, Calgary, AB.

Margrave G. F., L. Dong, P. Gibson, J. P Grossman, D. Henley and M. P. Lamoureux, 2003, Gabor deconvolution: Extending Wiener's Method to nonstationarity: CREWES Research Report, vol. **15**.